JOUL, Volume *2*

Supplemental Information

A Convergent Approach for a Deep Converting Lignin-First Biorefinery Rendering High-Energy-Density Drop-in Fuels

Zhengwen Cao, Michael Dierks, Matthew Thomas Clough, Ilton Barros Daltro de Castro, and Roberto Rinaldi

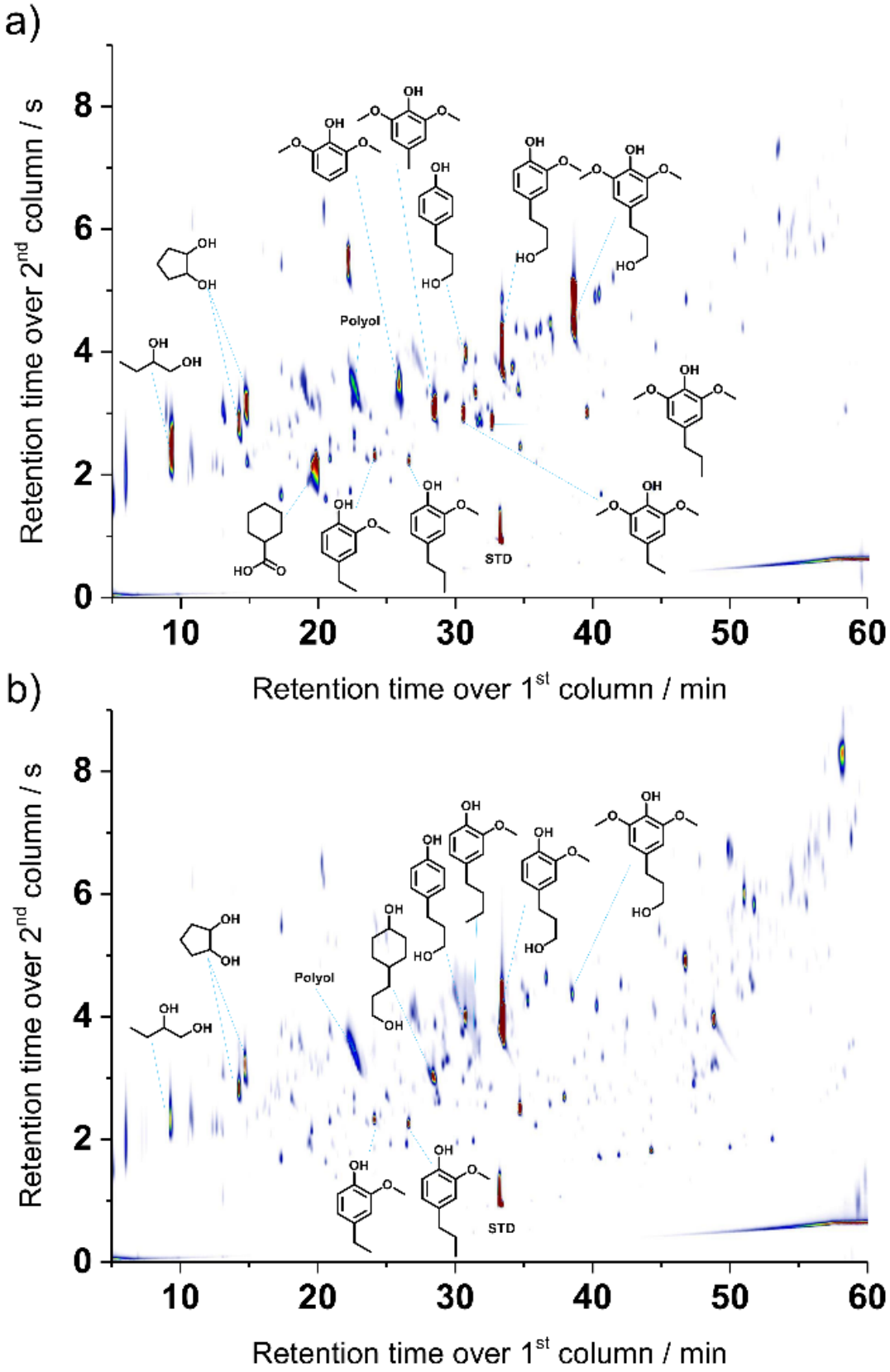

Figure S1. GC×GC−MS(FID) images showing volatile products of lignin oil from (a) Poplar and (b) Spruce.

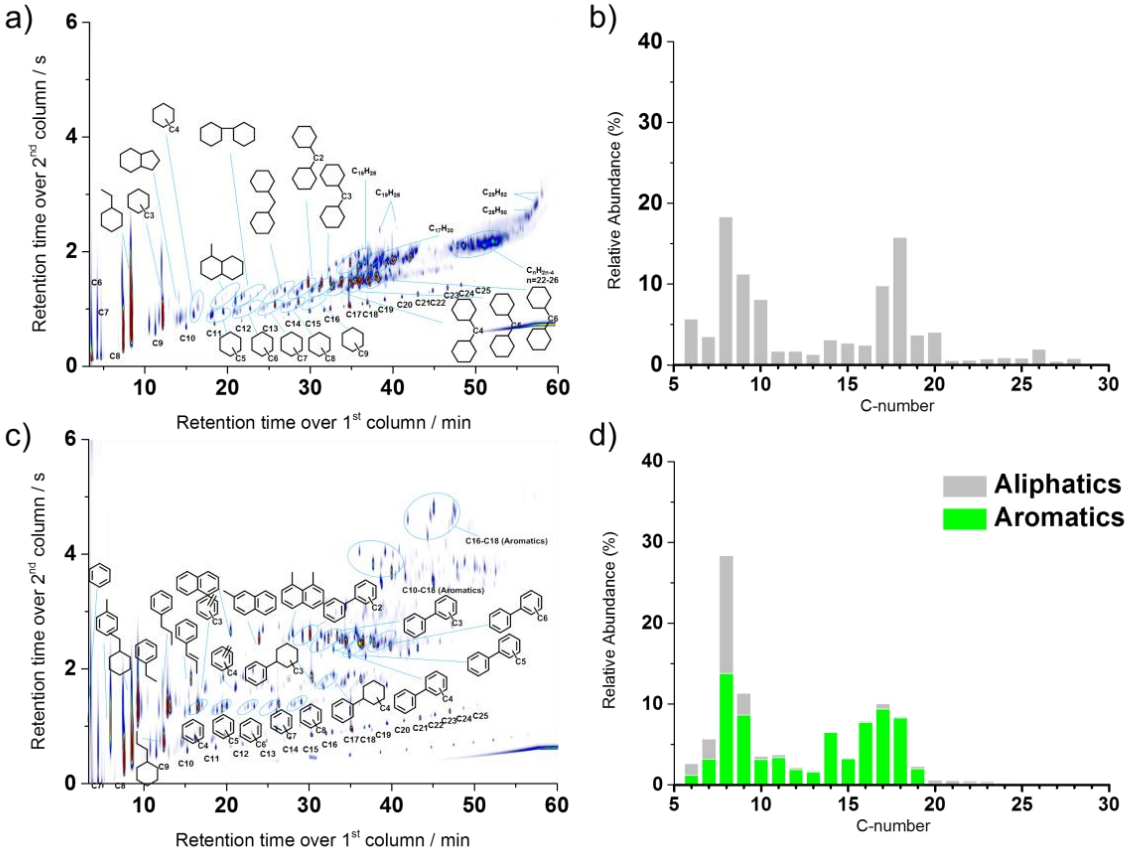

Figure S2. GC×GC−MS(FID) traces highlighting volatile products obtained from the HDO of Spruce (a, c). Distribution of products according their C-atoms (b, d). high pressure / 5 MPa - low temperature / 573 K for aliphatics-directed HDO; (c, d): low pressure / 1 MPa - high temperature / 623 K for aromatics-directed HDO. The semi-quantification of the products was performed based on ECN method.[1]

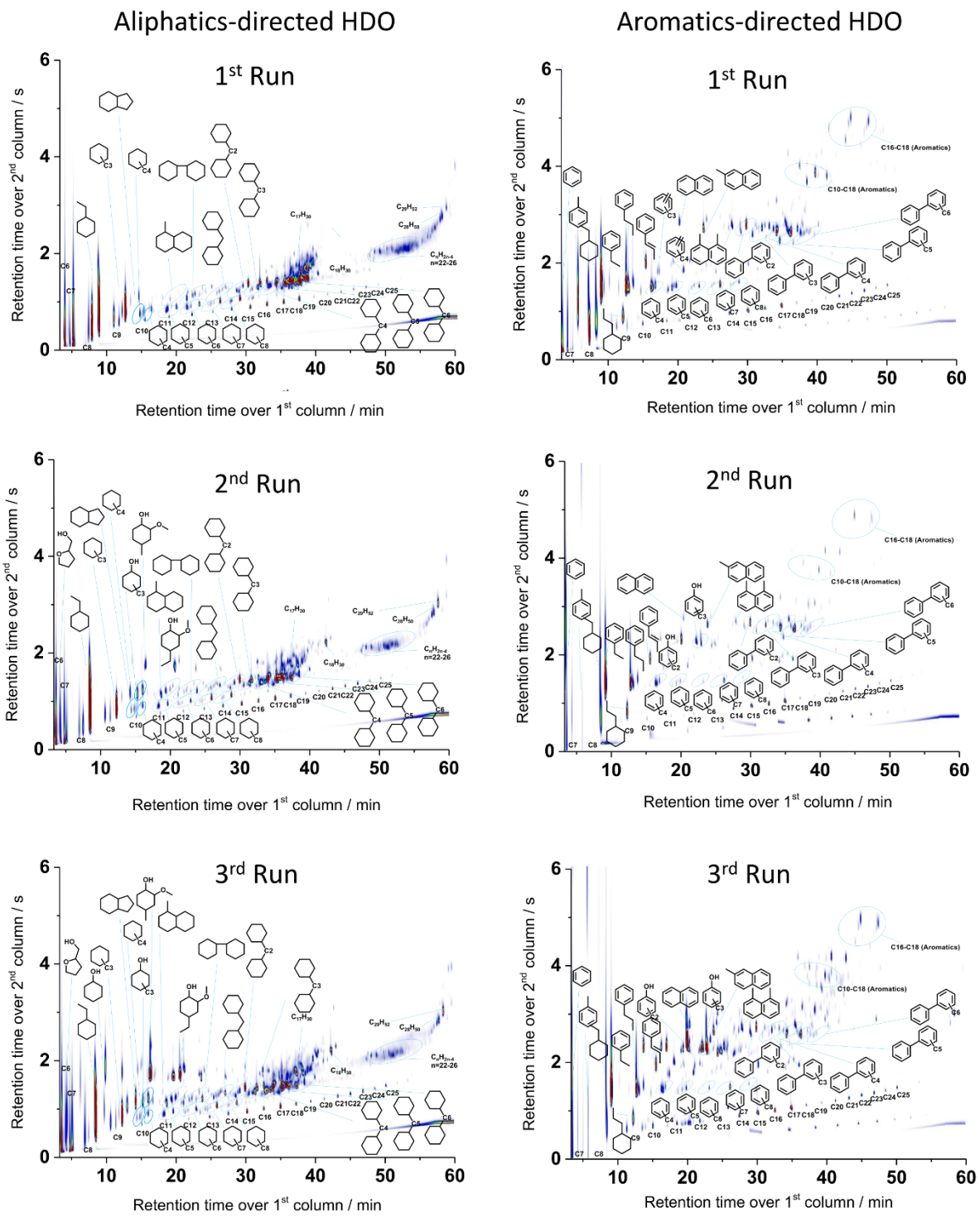

Figure S3. GC×GC–MS(FID) traces highlighting volatile products obtained from Poplar lignin oil in the recycling experiments under aliphatics-directed or aromatics-directed HDO condition.

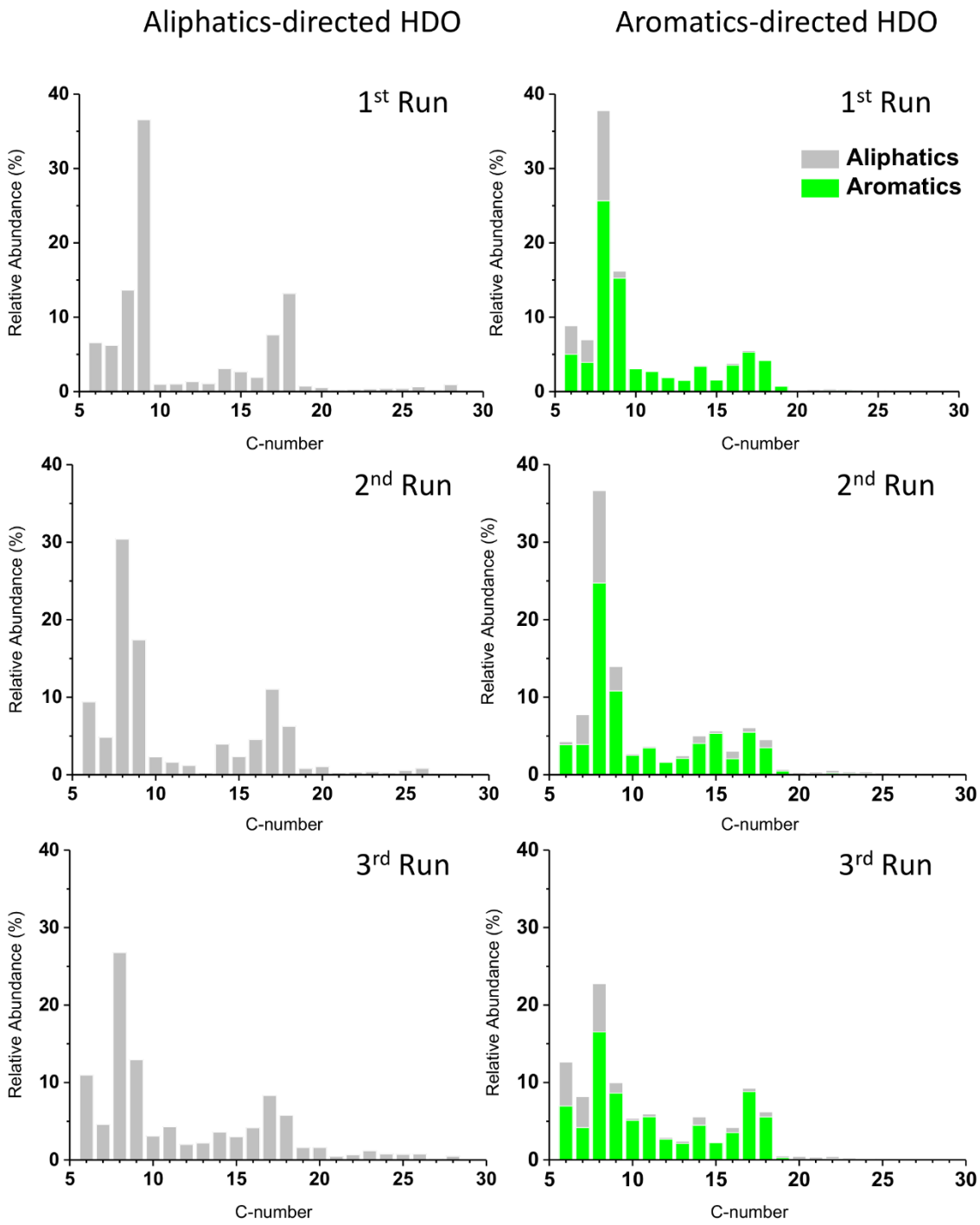

Figure S4. Product distribution in terms of C-number obtained from Poplar lignin oil in the recycling experiments under aliphatics-directed or aromatics-directed HDO condition. The semi-quantification of the products was performed based on ECN concept.[1]

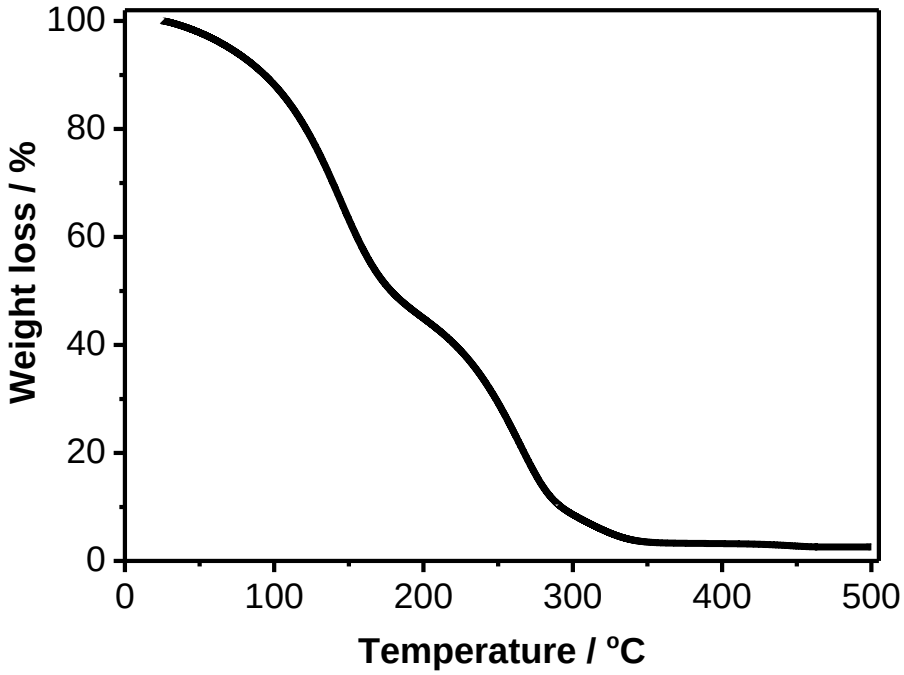

Figure S5. Temperature-ramped Thermogravimetric Analysis (TGA) traces products obtained from the HDO of Poplar.

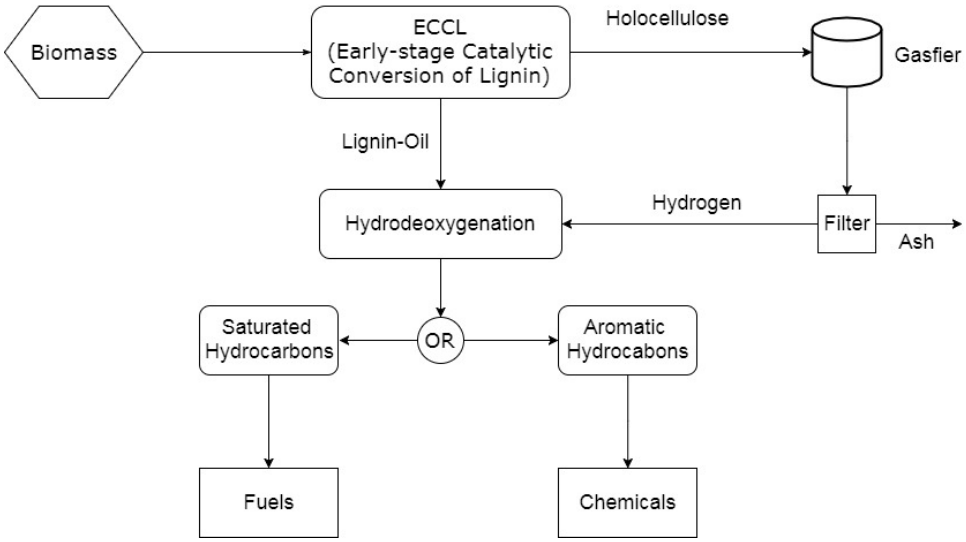

Figure S6. Block Flow Diagram for the proposed approach in this work

Table S1. Results of HDO of guaiacol in a two-run recycling experiment performed on the precursor Ni/SiO_2. Reaction conditions: 50 mg Ni/SiO_2, 5 mmol guaiacol, 9.5 ml *n*-octane, 568 K, 5 MPa H_2, 1h.

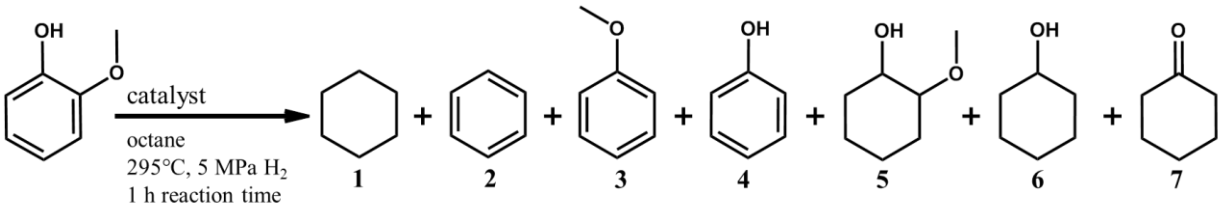

Catalyst	Run	Conversion (%)	Selectivity (%)						
			1	**2**	**3**	**4**	**5**	**6**	**7**
Ni/SiO_2 precursor	1	98	73	11	10	6	0	0	0
Ni/SiO_2 precursor	2	27	48	3	14	28	3	1	2

Table S2. Reported H_2-productivity in the gasification of cellulose, glucose, xylan, cedar wood, pine wood, and sawdust.

Entry	Feed	Catalyst	H_2 Productivity (H_2 mol/ feedstock kg)	Ref.
1	Cellulose	Ni-Zn-Al	18.7	[2]
2	Cellulose		11.5-14.0 (12.8) *	[3]
3	Cellulose	Ni/MCM-41	9.8-10.6 (10.2)	[4]
4	Cellulose	Ni-based	5-11 (8.0)	[5]
5	Cellulose	Ni/Zeolites	11.3-15.3 (13.3)	[6]
6	Cellulose	$Rh/CeO_2/SiO$	9.4-37.6 (23.5)	[7]
7	Glucose	Clostridium thermocellum	~4.5-12.8	[8]
8	Glucose	Ni-based/Al_2O_3	5.6-15.6	[9]
9	Xylan	Ni-Zn-Al	17.5	[2]
10	Xylan		9.0-18.0 (13.5)	[3]
11	Cedar wood	$Ni/CeO_2/Al_2O_3$	~28.0-35.0	[10]
12	Pine	Ni-based	70 (CO) †	[11]
13	Sawdust	Ni/MCM-41	~6.2-18.2	[12]

*the mean average value in parentheses is taken; †additional carbon monoxide is applied.

Table S3. Chemical compositions, theoretical carbon and weight yields, and corresponding 'process thermal efficiency' (PTE) values for selected biomass feedstocks.[13-15] The HHV values are relative to the products of the aliphatics-directed HDO.

Feedstock	Cellulose /%	Hemicellulose /%	Lignin /%	C- yield* /%	Weight yield /%	PTE (HHV)/%†
Cellulose to Ethanol (dry)				9	9[16,17]	13
NEW STRATEGY						
Sugarcane bagasse	42	25	20	21	13	30
Energy cane	43	24	22	23	15	33
Sweet sorghum	45	27	21	22	14	32
Hardwood						
Yellow-poplar	45	19	20	21	13	30
White poplar	52	23	16	17	11	24
White ash	41	15	26	28	17	39
Sand hickory	50	17	23	24	15	35
Boxelder	45	20	30	32	20	45
Scarlet oak	46	18	28	30	19	42
Northern red oak	46	22	24	25	16	36
River birch	41	23	21	22	14	32
Pacific madrone	44	23	21	22	14	32
Shagbark hickory	48	18	21	22	14	32
Softwood						
Pacific silver fir	44	10	29	31	19	44
White fir	49	6	28	30	19	42
Alligator juniper	40	5	34	36	23	51
Western larch	48	9	27	29	18	41
Sitka spruce	45	7	27	29	18	41

Table S3. *Cont.*

Feedstock	Cellulose /%	Hemicellulose /%	Lignin /%	C- yield* /%	Weight yield /%	PTE (HHV)/%†
Sand pine	44	11	27	29	18	41
Slash pine	46	11	27	29	18	41
Redwood	46	7	33	35	22	50
Second growth Northern white cedar	44	14	30	32	20	45
Western Hemlock	42	9	29	31	19	44

* For calculation of carbon yield, an average value of 50 wt% carbon in lignocellulose is taken,[13] and carbon loss during the HDO is also taken into account (according to equation 2). The presented value is for *fuel* production; for the chemical pathway, the value is lower by ~1%; † defined as 'process thermal efficiency' (PTE). 20 MJ kg^{-1}, an approximate average value is taken as the high heat value (HHV) for all varieties of biomass in this calculation, referring to [18]. The HHV values for biomass-to-ethanol and fuels obtained in our process are 30 and 45 MJ kg^{-1} (referring to *Fischer-Tropsch* diesel), respectively.[15]

References

1. Scanlon, J.T., and Willis, D.E. (1985). Calculation of flame ionization detector relative response factors using the effective carbon number concept. J Chromatogr Sci *23*, 333-340.
2. Wu, C., Wang, Z., Huang, J., and Williams, P.T. (2013). Pyrolysis/gasification of cellulose, hemicellulose and lignin for hydrogen production in the presence of various nickel-based catalysts. Fuel *106*, 697-706.
3. Couhert, C., Commandre, J.-M., and Salvador, S. (2009). Is it possible to predict gas yields of any biomass after rapid pyrolysis at high temperature from its composition in cellulose, hemicellulose and lignin? Fuel *88*, 408-417.
4. Zhao, M., Florin, N.H., and Harris, A.T. (2009). The influence of supported Ni catalysts on the product gas distribution and H2 yield during cellulose pyrolysis. Appl Catal B: Environ *92*, 185-193.
5. Taylor, A.D., DiLeo, G.J., and Sun, K. (2009). Hydrogen production and performance of nickel based catalysts synthesized using supercritical fluids for the gasification of biomass. Appl Catal B: Environ *93*, 126-133.
6. Inaba, M., Murata, K., Saito, M., and Takahara, I. (2006). Hydrogen production by gasification of cellulose over Ni catalysts supported on zeolites. Energy Fuels *20*, 432-438.
7. Asadullah, M., Ito, S.I., Kunimori, K., Yamada, M., and Tomishige, K. (2002). Biomass gasification to hydrogen and syngas at low temperature: Novel catalytic system using fluidized-bed reactor. J Catal *208*, 255-259.
8. Levin, D.B., Islam, R., Cicek, N., and Sparling, R. (2006). Hydrogen production by Clostridium thermocellum 27405 from cellulosic biomass substrates. Int J Hydrogen Energ *31*, 1496-1503.
9. Li, S., Lu, Y., Guo, L., and Zhang, X. (2011). Hydrogen production by biomass gasification in supercritical water with bimetallic Ni-M/γAl2O3 catalysts (M = Cu, Co and Sn). Inter J Hydrogen Energ *36*, 14391-14400.
10. Kimura, T., Miyazawa, T., Nishikawa, J., Kado, S., Okumura, K., Miyao, T., Naito, S., Kunimori, K., and Tomishige, K. (2006). Development of Ni catalysts for tar removal by steam gasification of biomass. Appl Catal B: Environ *68*, 160-170.
11. Corella, J., Aznar, M.P., Caballero, M.A., Molina, G., and Toledo, J.M. (2008). 140 g H2/kg biomass d.a.f. by a CO-shift reactor downstream from a FB biomass gasifier and a catalytic steam reformer. Inter J Hydrogen Energ *33*, 1820-1826.
12. Wu, C., Wang, L., Williams, P.T., Shi, J., and Huang, J. (2011). Hydrogen production from biomass gasification with Ni/MCM-41 catalysts: Influence of Ni content. Appl Catal B: Environ *108–109*, 6-13.
13. Pettersen, R.C. (1984). The chemical composition of wood. The chemistry of solid wood *207*, 57-126.

14. Kim, M., and Day, D.F. (2011). Composition of sugar cane, energy cane, and sweet sorghum suitable for ethanol production at Louisiana sugar mills. J Ind Microbiol Biotechnol *38*, 803-807.

15. Argonne National Laboratory (2010). Lower and Higher Heating Values of Gas, Liquid and Solid Fuels. Lower and Higher Heating Values of Gas, Liquid and Solid Fuels.

16. Harris, J.F., Baker, A.J., Conner, A.H., Jeffries, T.W., Minor, J.L., Pettersen, R.C., Scott, R.W., Springer, E.L., Wegner, T.H., and Zerbe, J.I. (1985). Two-stage, dilute sulfuric acid hydrolysis of wood: an investigation of fundamentals.

17. Rinaldi, R., and Schuth, F. (2009). Design of solid catalysts for the conversion of biomass. Energy Environ Sci *2*, 610-626.

18. Demirel, Y. (2012). Energy Energy Types. 27-70.